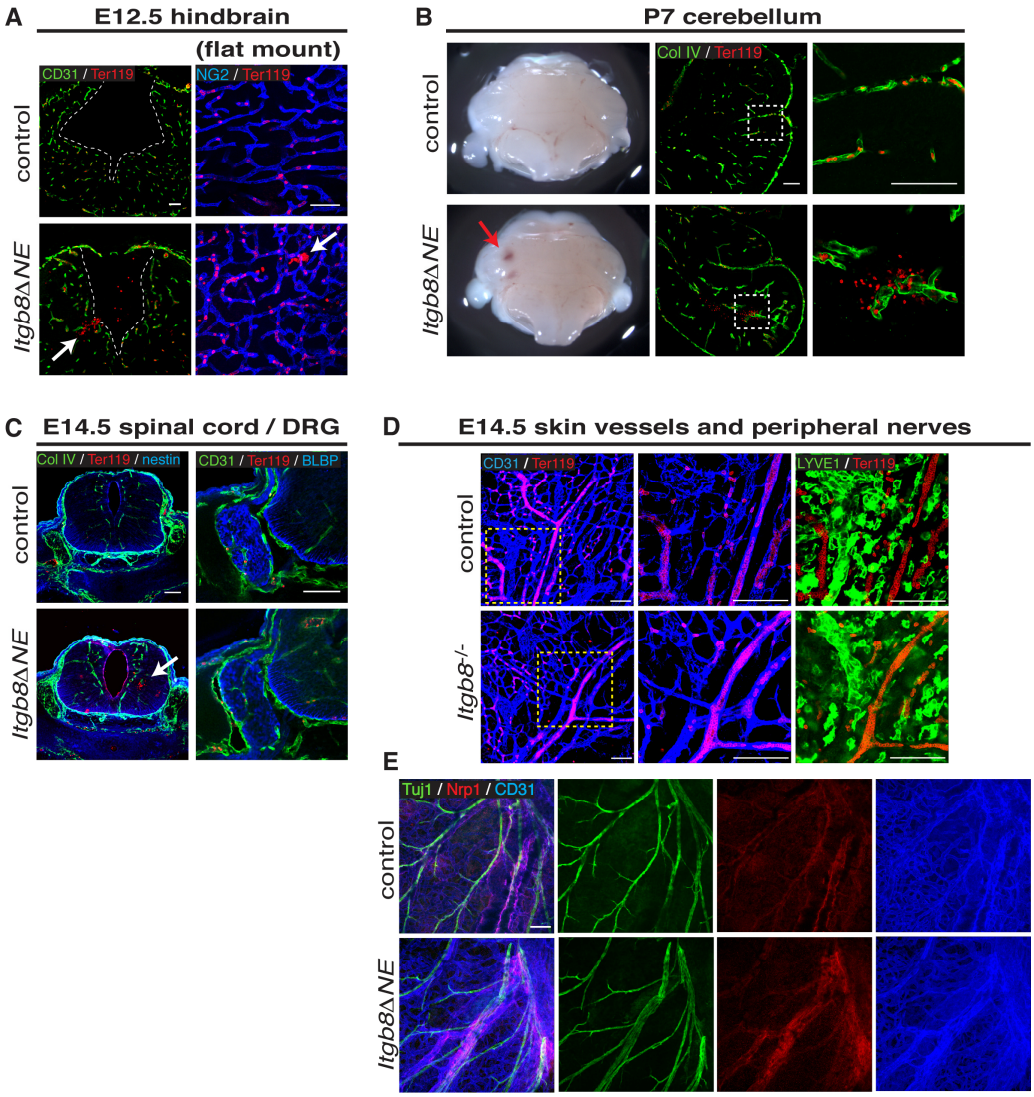

Supplementary Figure 1. Deletion of *Itgb8* in the neuroepithelium of the hindbrain, spinal cord and neonatal cerebellum, but not peripheral nervous system results in vascular irregularities and hemorrhage. A) Visualization at E12.5 of blood vessels (endothelial cell-specific CD31, green or pericyte-specific NG2, blue) and red blood cells (Ter119, red) in coronal sections (left) and flatmounts (right) of hindbrains reveals dysplastic vessels and hemorrhage (arrows) localized to the ventral hindbrain subventricular zone neuroepithelium. **B)** (Left) Punctate hemorrhage (arrow) is apparent in the cerebella of *Itgb8ΔNE* mutants, but not controls at P7. (Middle) Visualization at P7 of vasculature (collagen IV, green) and red blood cells (Ter119, red) in sagittal cerebellar sections reveals the presence of tortuous vessels and localized bleeding in a mutant that are not present in controls. Higher magnification insets are to the right. **C)** (Left) Visualization in E14.5 spinal cord of radial glia (nestin, blue), red blood cells (Ter119, red) and blood vessels (Col IV, green) reveal dysplastic vessels and associated hemorrhage (arrow) not present in controls. (Right) Visualization in E14.5 dorsal root ganglia (DRG) sections of brain lipid- binding protein (BLBP, blue), CD31 (green) and Ter119 (red) indicates that the

vasculature appears to be normal without hemorrhage in controls and mutants. **D)** Visualization at E14.5 of blood vessels (CD31, blue), lymphatic vessels (LYVE-1, green) and red blood cells (Ter119, red) reveal absence of hemorrhage and normal vascular and lymphatic anatomies in forelimb skin of both *Itgb8* knockout mutant and control embryos. Right two panel sets are higher magnification insets of boxed areas in left in middle panels. **E)** Staining forelimb skin for vessels (CD31, blue) and peripheral nerves (Tuj1, green) reveals normal vessel-nerve alignment. Additional staining with anti-Nrp1 (red) reveals normal peripheral nerve-mediated arteriogenesis in the absence of *Itgb8.* N > 4 for all observations. Scale bars: 100 μm.

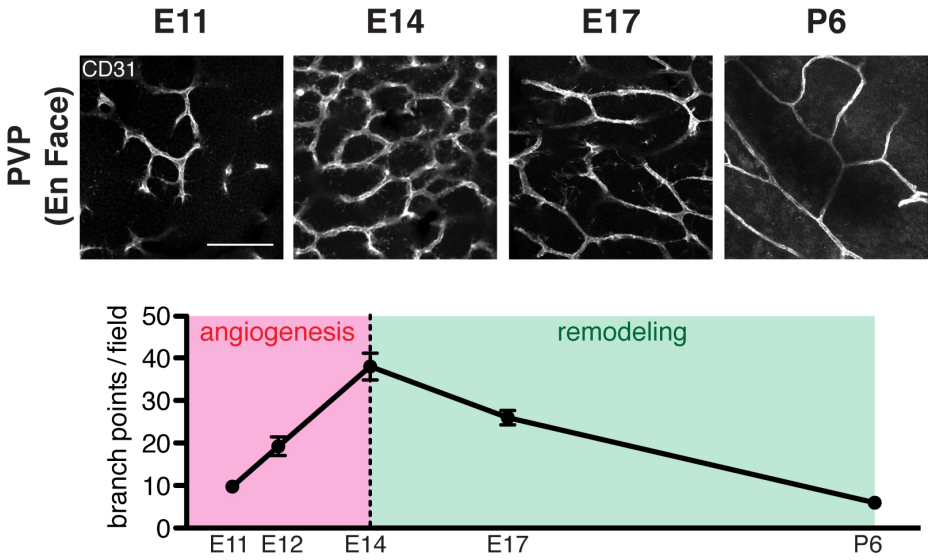

Supplementary Figure 2. Vascular branching over time. Top: Brains at indicated time points were stained for vessels (anti-CD31, white), flatmounted and imaged at the level of the periventricular vascular plexus (PVP). **Bottom:** The number of branch points per field was quantified at indicated time points, revealing increases in density of branch points in the PVP from embryonic day (E)11 to E14 (angiogenic growth) followed by a reduction in density from E14 to postnatal day (P)6. Since the brain is rapidly expanding between E14 and P6, the decreased density probably does not reflect reduced total number of branch points. N = 4 at each time point. Error bars, s.e.m. Scale bar: 100 μm.

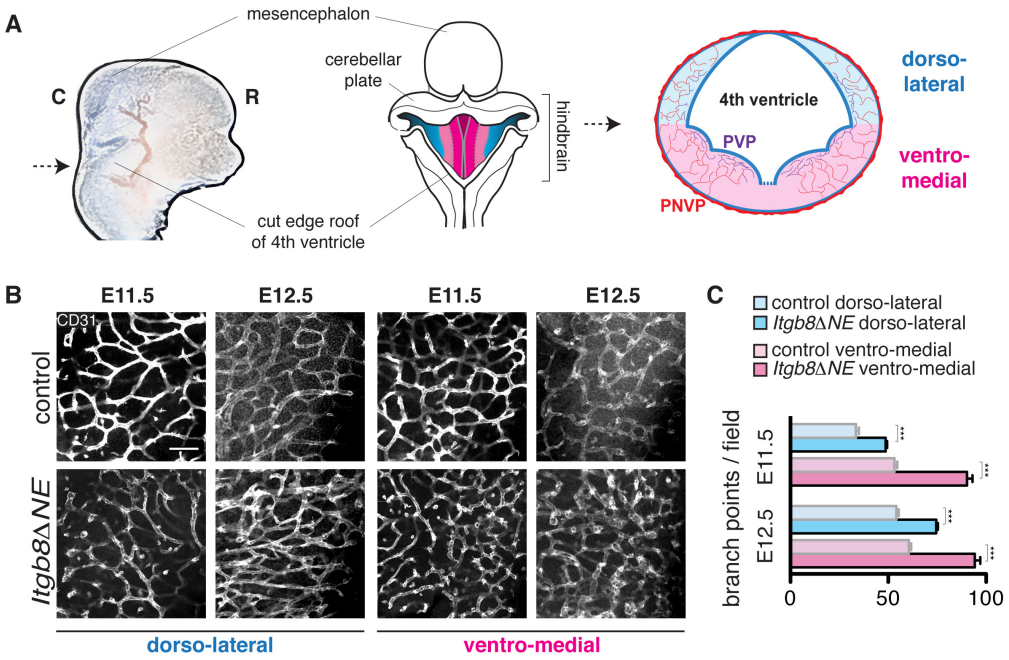

Supplementary Figure 3. Increased vascular branching in hindbrain neuroepithelium of *Itgb8ΔNE* mutants. A) Diagram illustrating flat-mount preparations used to analyze domain-specific branching morphogenesis in the developing hindbrain as previously described (H. Gerhardt, C. Ruhrberg, A. Abramsson, H. Fujisawa, *et al.*, *Dev Dyn* **231**, 503-9 (2004).). C = caudal; R = rostral; PVP = periventricular vascular plexus; PNVP = Perineural Vascular Plexus. **B)** The vasculature in the PVP of E11.5 and E12.5 control and mutant hindbrains were visualized using anti-CD31. Scale bar: 100μm. **C)** Quantitative analysis of vascular branchpoints in the dorso-lateral and ventro-medial domains reveals a spatio-temporal gradient of branching vascular morphogenesis with increased branch point densities in both regions at each time in the *Itgb8ΔNE* mutants. P values from Student's *t* test: *** P < 0.0005. N = 4 controls, 4 mutants at each time point. Error bars, s.e.m.

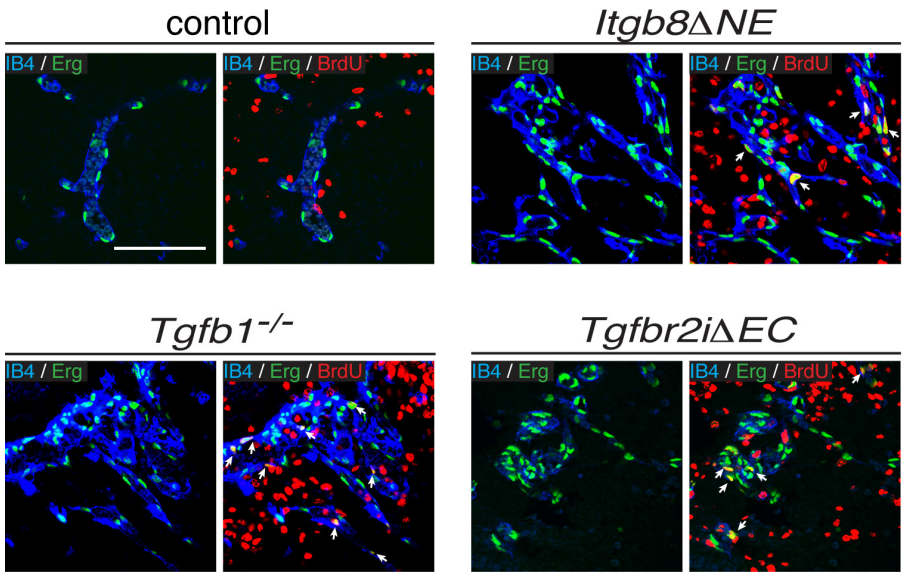

Supplementary Figure 4. Increased endothelial cell number and proliferation in *Itgb8ΔNE* and TGFβ mutants. Pregnant mares were injected with 10µg/g BrdU body weight 2 hours prior to harvesting embryos. 15µm cryosections were stained for BrdU (proliferating nuclei; red), isolectin B4 (vessels; blue), and Erg (endothelial cell nuclei; green). Arrows indicate BrdU/IB4/Erg triple-positive cells. N = 4 for each genotype. Scale bars: 100 µm. Quantification of endothelial cell nuclei density and proliferation is presented in Figures 2c and Figure 5.

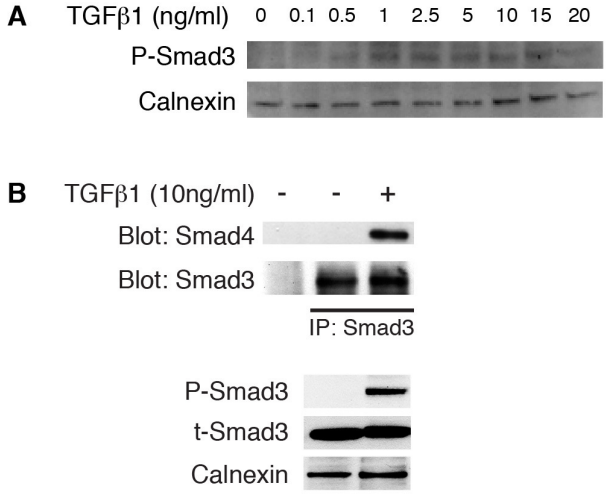

Supplementary Figure 5. TGFβ1 stimulates phosphorylation of Smad3 and association with Smad4 in MS-1 endothelial cells. A. Does titration of TGFβ1 in MS1 cells revealed peak phosphorylation of Smad3 at 10ng/ml TGFβ1. B. Smad3-Smad4 association was revealed by immune-precipitation (IP) at this concentration. N = 4.

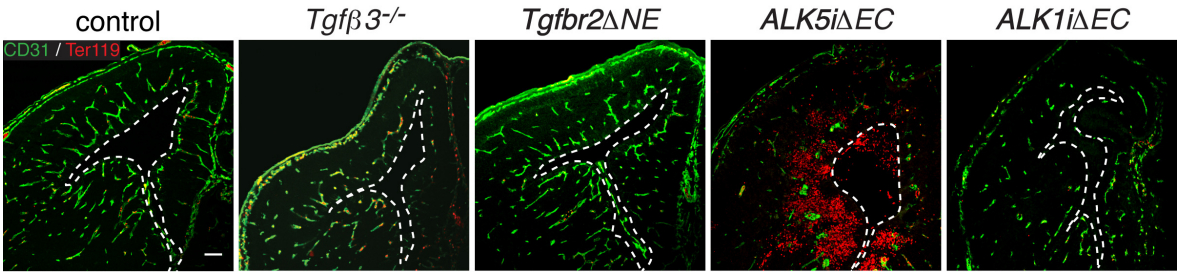

Supplementary Figure 6. Vascular and hemorrhagic phenotypes in *Tgfb3*$^{-/-}$, *Tgfbr2ΔNE*, *Alk1iΔEC*, and *Alk5iΔEC* mutant mice. E14.5 coronal brain sections from indicated mutant and control mice were stained for vascular endothelial cells (anti-CD31, green) and red blood cells (Ter119, red). Vascular morphology appeared normal and hemorrhage was absent (no extraluminal red blood cells) in *Tgfb3*$^{-/-}$, *Tgfbr2ΔNE*, and *Alk1iΔEC* mutants compared to controls. In contrast, endothelial cell-specific deletion of Alk5 (*Alk5iΔEC*) resulted in a very similar phenotype including vascular malformations and diffuse hemorrhage as observed *Itgb8ΔNE,* *Tgfb1*$^{-/-}$*,* and *Tgfbr2iΔEC* mice. N = 4 for each genotype. Scale bar: 100 μm.

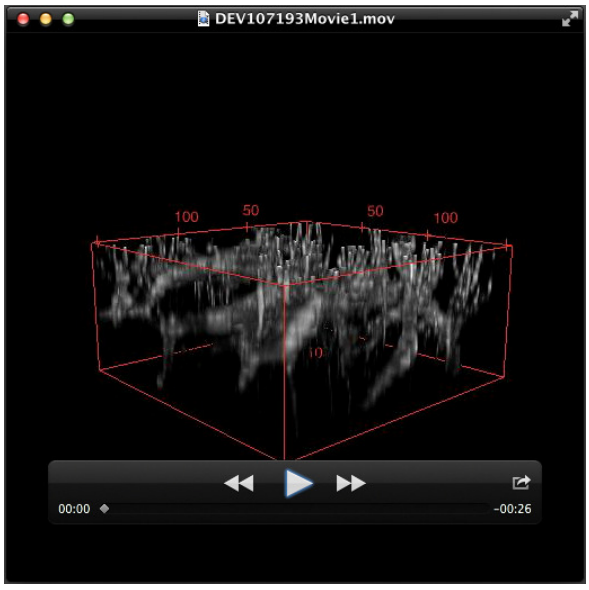

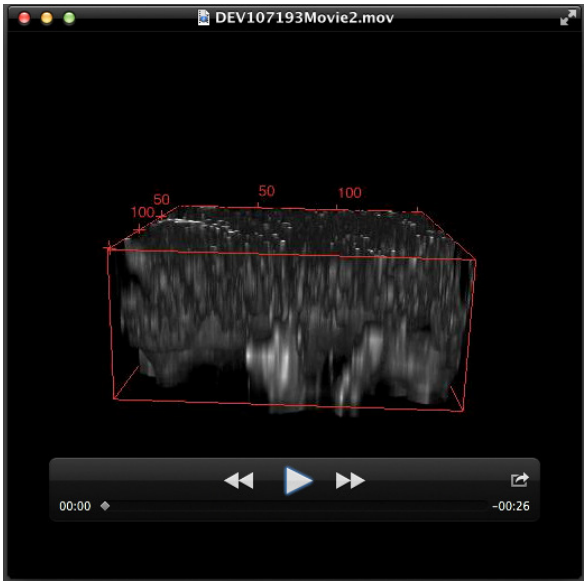

Supplementary Movies. Comparison of vascular sprouting in control (1) and *Itgb8ΔNE* mutants (2). Three-dimensional projections through periventricular vascular plexus (between levels 1 and 2 in Figure 2a) of E11.5 flat-mounted control and *Itgb8ΔNE* forebrains in the ventral telencephalon. At this stage, most vascular filopodia project to the ventricular surface (top of rotating image block), with a minority of filopodia extending between interconnecting vessels. Compared to controls, mutants have a dramatic increase in the density of filopodial sprouts extending towards the ventricular surface.